

MODELING AND SIMULATION OF BALISE UP-LINK DATA TRANSMISSION BASED ON FINITE ELEMENT METHOD

LINHAI ZHAO*, YING JIANG

School of Electronics and Information Engineering, Beijing Jiaotong University, Beijing 100044, China

ABSTRACT

The balise is an important component in train operation control system fulfilling the task of Ground-Train Point-Mode data transmission. This paper presents a finite element based method for researching the electromagnetic interaction process of balise up-link data transmission with respect to the basic theoretical level. Based on the basic structure and working principle of balise information transmission system, the model of balise up-link data transmission is built by employing the finite element method. Through simulation, the overall electromagnetic field distribution of this interaction process is obtained. By means of contrast verification using simulation results and practical data, the validity and credibility of this FEM based model is proved in two perspectives, which will provide theoretical foundations for further researches in terms of balise information transmission.

Keywords: *Balise Transmission Module Antenna, Finite Element Method, Balise Up-link Data Transmission, Electromagnetic Interaction Process*

1. INTRODUCTION

The traffic safety in railway lines is guaranteed by applying the corresponding train operation control system. As key component of this system, the balise information transmitting subsystem, comprised of on-board Balise Transmission Module (BTM) and ground balise, mainly accomplishes the Ground-Train Point-Mode data transmission of balise up-link signal which contains crucial information (e.g., temporary speed limitation, geographical position and ground circumstances) for speed control of the train. With the railways developing more rapidly, the train operation speed is increasing much faster, which demands even higher requirements for the transmission quality of balise information. Therefore, it is necessary to perform the modeling and simulation of Balise Up-link Data Transmission (BUDT) from basic theoretical level point of view.

Currently, researches regarding the balise mainly concentrate on placement optimization, reliability and fault analysis, crosstalk reduction, testing methods, etc. M. Sandidzadh [1] found out the optimum places of balises in the line to reduce tachometer errors by combining Genetic Algorithm and Kalman filter concepts. In consideration of the influences of electromagnetic factors and radio frequency (RF) design factors, the reliability targets of balise transmission system are analyzed [2], and by means of FTA (Fault Tree Analysis) and FMEA (Failure Mode and Effect Analysis), J. del Portillo [3] designed a suitable topology to accomplish

safety requirements for the on-board front-end transceiver of BTM. R. Sharma [4] analyzed the range of crosstalk problems encountered with the major trackside equipment, i.e., the balise and the loops. H. Zhao demonstrated that the dynamic characteristics of BTM could be modeled at four resolution layers, ranging from low to very high resolution [5], and based on that, the adaptability evaluation method for high speed circumstances was proposed [6]. By employing methods of RF, spectrum analysis and virtual instrument technique, the on-line testing of balises could be achieved [7].

In summary, with respect to the modeling and simulation of BUDT under train movement conditions, few reports related have been published up to now, mainly owing to the fact that the immense and complex solution domain of this electromagnetic interaction process is so difficult to solve. Fortunately, finite element method (FEM) happens to be advantageous on this issue, as it is a highly effective numerical computing method. Hence, based on finite element technique and starting from electromagnetic RF excitation angle, the modeling and simulation of BUDT is carried out. Simulation and experimental results show that the BUDT can be well simulated with the use of FEM, thus providing conveniences for further studies such as transmission optimization.

2. BASIC STRUCTURE AND WORKING PRINCIPLE OF BALISE INFORMATION TRANSMISSION SYSTEM

As illustrated in Figure 1 is the basic structure of balise information transmission system, which mainly includes the on-board BTM device and ground balise. Among them, the BTM device is comprised of the down-link excitation signal generator and the associated sending antenna, up-link signal receiving antenna and telegram processing module; while the balise consists of down-link signal receiving antenna, telegram storage, telegram sending module and the associated sending antenna, etc.

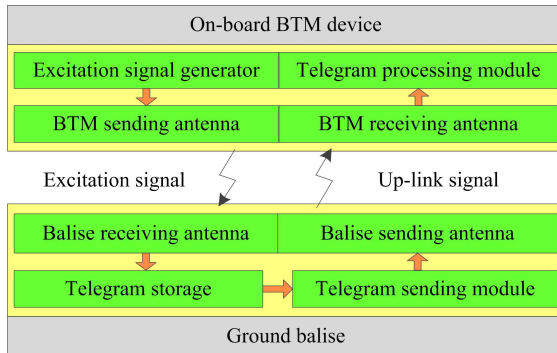


Figure 1: Basic Structure Of Balise Information Transmission System

Most of the time, the ground balise is in dormant mode, and the down-link excitation signal generator of on-board BTM device will always radiate RF signals downwards via BTM sending antenna, which forms a high frequency electromagnetic field covering the entire Ground-Train space. When a train approaches the balise within a certain distance, through electromagnetic induction, the induced voltage in balise receiving antenna will gradually increase and finally exceed the predefined threshold, thereby activating the balise, and afterwards, the telegram sending module starts to work, reading telegram information stored in the memory, modulating them into up-link signal with specific formats and sending them out in certain transmission rate. At the same time, the receiving antenna of on-board BTM device would induce the telegram signal transmitted by ground balise. After signal conditioning, filtering, demodulation, decoding and other procedures, the information contained in the signal is then extracted and sent to Vital Computer for train operation control. With the train passing and leaving the balise out of a certain distance, the down-link induced voltage within ground balise is below the threshold, which makes balise go into dormancy again.

3. MODELING OF BUDT BASED ON FEM

3.1 Mathematical Model of Balise Up-link Signal

With references to balise technical specification [8], the mathematical model of balise up-link signal is characterized in Figure 2.

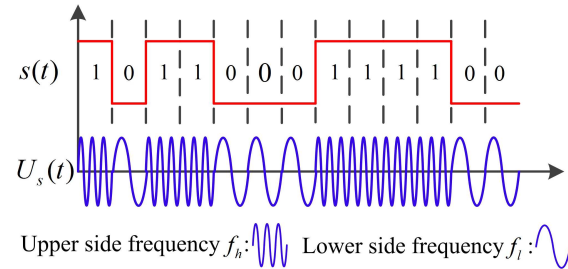


Figure 2: Basic Up-Link Signal

The mathematical expression is described as:

$$U_s(t) = A_s \cos(2\pi f_c t + 2\pi \Delta f \int s(t) dt + \varphi_0) \quad (1)$$

Where A_s denotes the signal amplitude, f_c refers to the carrier frequency, Δf is frequency deviation, $s(t)$ represents the code sequence of telegram signal and takes alternative values between logic “1” and logic “0”, which corresponds to upper side frequency $f_h = f_c + \Delta f$ and lower side frequency $f_l = f_c - \Delta f$ respectively, and φ_0 stands for the initial phase of the signal. The main frequency parameters and the associated error ranges are listed in Table 1.

Table 1

Frequency values and admissible errors of up-link signal

	Standard value	Admissible error
carrier frequency f_c	4.234MHz	± 20 kHz
frequency deviation Δf	282.24kHz	± 3 kHz
upper side frequency f_h	4.516MHz	± 20 kHz
lower side frequency f_l	3.951MHz	± 20 kHz
transmission rate	564.48kbit/s	± 14.11 kbit/s

3.2 Establishment of Balise Dynamic Transmission Model Based on FEM

The basic theory of FEM is to segment the solution domain into a lot of small subdomains termed as “finite element”. By applying certain solving methods to each subdomain and summing the derived results of all subdomains, the solution to original domain is then attained. Since BUDT is a time-varying motion process, it is suggested that three-dimensional transient electromagnetic field method be used to solve this problem which will then be divided into two transient processes for the sake of clarity and simplicity, i.e., the transient

mechanical motion process and the transient electromagnetic interaction process.

When dealing with mechanical motion process, the local subdivision method is adopted to compute the effects brought by three-dimensional transient motion. Here, the discretization for displacement x is introduced for computation and the discrete format is given by the following equation:

$$\left\{ \frac{dx}{dt} \right\}^{t+\Delta t} = \frac{\{x^{t+\Delta t}\} - \{x^t\}}{\Delta t} \quad (1)$$

As for electromagnetic interaction process, since the frequency of balise up-link signal is relatively low, the Maxwell Equations for solving this electromagnetic process can be written as

$$\begin{cases} \nabla \times H = \sigma E \\ \nabla \times E = \frac{\partial B}{\partial t} \\ \nabla \cdot B = 0 \end{cases} \quad (2)$$

Where H denotes the magnetic-field strength, B the magnetic density and E the electrical field strength.

In this FEM based model of BUDT, the voltage source fed to balise coil is the excitation. Since the balise coil belongs to entity winding, its resistance is related to many factors such as frequency and material, so Skin Effect needs to be taken into account, and also for this reason it should be treated as AC resistance R . When applying voltage source V , the AC resistance of the winding is still unknown and could be computed using the following equation:

$$V = \iiint_R J(E + v \times B) dR \quad (3)$$

Where J denotes the current density vector of the excitation coil, v is the translation speed of the motion region in this model, and refers to train operation speed in this paper.

In general, the analysis and computation of the electromagnetic field are achieved by means of solving differential equations. For ordinary differential equations, the solution is uniquely determined as soon as the supplementary conditions which mainly refer to the ambient physical circumstances of the solution domain, i.e., the boundary conditions are specified.

With employment of equations (1), (2), (3) and other principles mentioned above, the FEM based model of BUDT is built and displayed in Figure 3. The model size, frame structure, and excitation values are all in accordance with those of practical conditions.

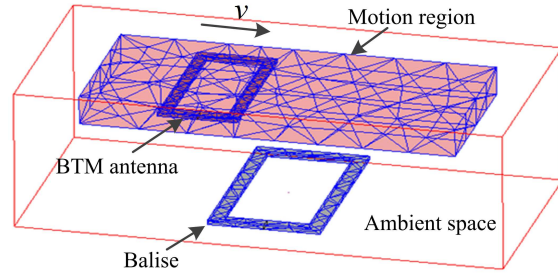


Figure 3: FEM based model of BUDT

The model mainly consists of balise and BTM coil, referring to sending and receiving antenna of up-link data transmission, respectively. The semi-transparent rectangular box surrounding BTM antenna is the motion region of the model, representing the running range of train, and the transparent air box represents the outermost layer of the model. When implementing the simulation using FEM based software, with regard to the meshing density, the corresponding settings should be performed according to different requirements for solution precisions. Since the most prevalent way for three-dimensional meshing now is to adopt tetrahedral elements, which is simple and stable, and hence, the meshing for balise and BTM antennas is set pretty dense due to its high requirements of calculation accuracy, while the meshing for motion region is relatively sparse.

4. SIMULATION OF BUDT

According to the requirements prescribed in balise testing specification [9], the size parameters and up-link signal (also termed as input signal) are applied to the FEM model built in Figure 3, herein and after, all the parameters and excitation signals are referred to as simulation conditions.

4.1 Input Signal of BUDT Model

To simulate the working conditions of BUDT system under train movement conditions, first the telegram signal is fed to balise as the input signal, while the BTM antenna is only able to translate in a velocity of v without any excitation, as it is able to induce voltage signals through electromagnetic induction. The parameters of input signal in this model is illustrated in Figure 4(a), 4(b) and 4(c), corresponding to telegram code sequence, time-domain waveform and spectrum, respectively.

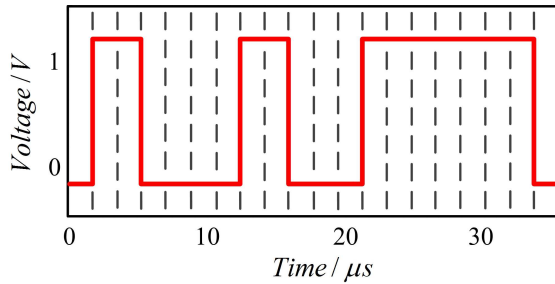


Figure 4(a) Code sequence of input signal

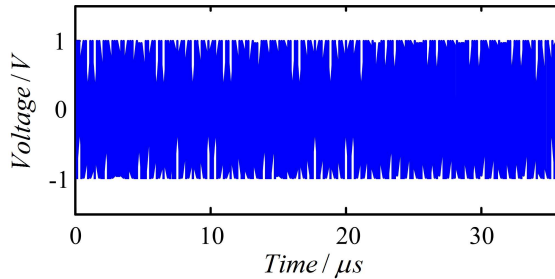


Figure 4(b) Waveform of input signal

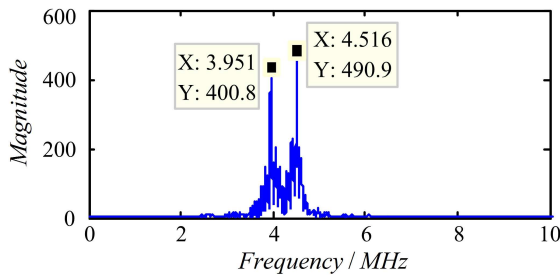


Figure 4(c) Spectrum of input signal

Figure 4 Corresponding parameters of the input signal

As shown in Figure 4(a) is the code sequence of input signal, which is formed of 20 bits, i.e.,

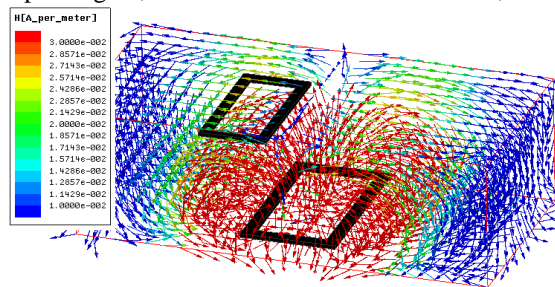
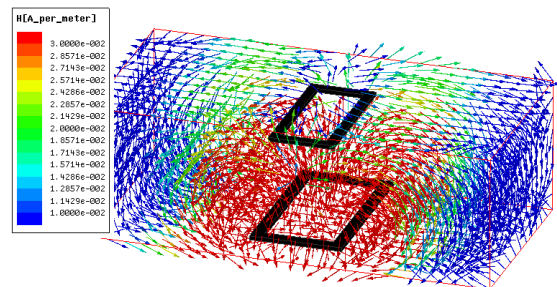
Figure 5(a) Overall electromagnetic distribution when $\Delta x = -150\text{mm}$ Figure 5(b) Overall electromagnetic distribution when $\Delta x = 0$

Figure 5 Overall Electromagnetic Distributions With Different Positions Of BTM Antenna

The density of magnetic induction line is advised to visually depict the strength of electromagnetic distributions. As can be seen from both Figure 5(a) and 5(b), the magnetic induction line is pretty dense nearby balise and relatively sparse at the vicinity of BTM antenna and even sparser in the ambient space. And consequently, it could be inferred that

[0 1 1 0 0 0 1 1 0 0 0 1 1 1 1 1 1 1 0] and refers to the telegram information transmitted upwards. It is observed from Figure 4(b) that the time-domain waveform of up-link signal is essentially an equal-amplitude sinusoidal wave. As demonstrated in Figure 4(c) is the spectrum derived from the input signal by means of Fourier Transform, it has two peaks in frequency domain, corresponding to lower side frequency f_l and upper side frequency f_h , respectively. It could be seen that the height of the peak attached to upper side frequency is greater than that of lower side frequency, which is in conformity to the situation in Figure 4(a) where the time of logic "1" lasts longer than that of logic "0".

4.2 Electromagnetic Distribution within BUDT Model

Suppose the horizontal distance between the centers of BTM antenna and balise is Δx , let $\Delta x = -150\text{mm}$ and $\Delta x = 0$ respectively, and the corresponding simulation results of the overall electromagnetic distributions of BUDT at two different positions are shown in Figure 5(a) and 5(b).

the electromagnetic field strength nearby balise is the strongest, because it's the only signal source within the model, while the electromagnetic field strength at the vicinity of BTM antenna takes the second place mainly attributes to its ability to induce voltage signal. And due to the fact that the

distance is too far away, the electromagnetic field strength in the ambient space is the weakest.

For a more comprehensive cognition of the overall electromagnetic field strength distribution

of this process, a cross-sectional view of the electromagnetic field strength on BTM surface is displayed in Figure 6(a) and 6(b).

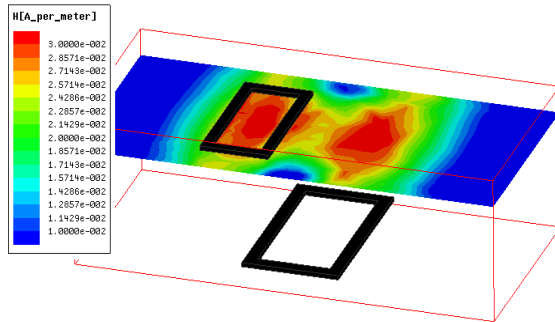


Figure 6(a) Electromagnetic distribution on BTM surface when $\Delta x = -150\text{mm}$

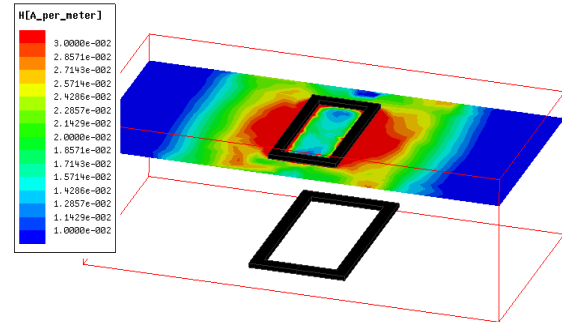


Figure 6(b) Electromagnetic distribution on BTM surface when $\Delta x = 0$

Figure 6 Electromagnetic Distributions On BTM Surface

With careful observation, a slight difference could be noted between the two Figures. In Figure 6(a), there are two areas (i.e., right above the balise and at the vicinity of BTM antenna) where the electromagnetic field strength is relatively strong, while in Figure 6(b) there is only one such area (around BTM antenna). The reason for this difference mainly lies in the horizontal distance between balise and BTM antenna. Specifically, when BTM antenna is far away from balise, the coupling coefficient between them is quite weak, as a consequence, the magnetic field distribution is mainly determined by the excitation source; however, when BTM antenna gets quite close to balise, it is able to induce relatively strong voltage signal through electromagnetic induction, which would somehow change the original magnetic distribution in turn.

5. EXPERIMENTAL VERIFICATION

To ensure the validity and credibility of the FEM based model, with the use of simulation results and practical data, contrast verification is carried out from two perspectives of BTM voltages, i.e., static induced voltage (SIV) and dynamic induced voltage (DIV).

5.1 Verification of SIV

For the purpose of acquiring SIV at one fixed position within a period of time, set $\Delta x = 0$ where BTM antenna is fixed right above the balise and apply the identical simulation conditions described above to the model. The simulation results obtained are illustrated in Figure 7(a), 7(c), 7(e) and 7(g); while the corresponding practical data are illustrated in parallel in Figure 7(b), 7(d), 7(f) and 7(h) as contrast.

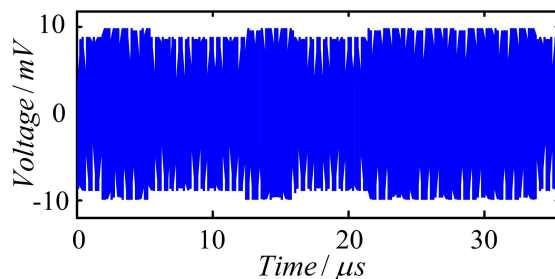


Figure 7(a) Waveform of simulated SIV

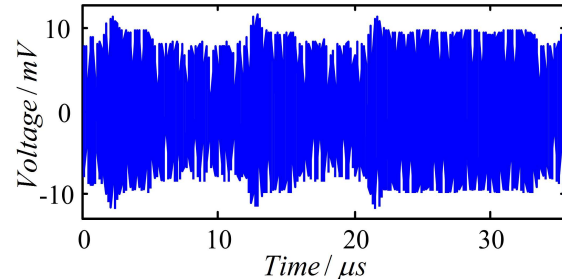


Figure 7(b) Waveform of practical SIV

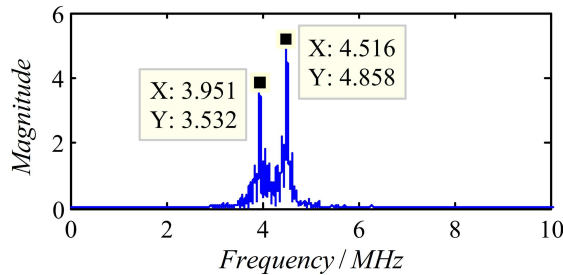


Figure 7(c) Spectrum of simulated SIV

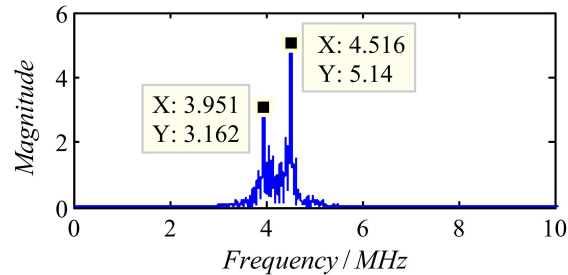


Figure 7(d) Spectrum of practical SIV

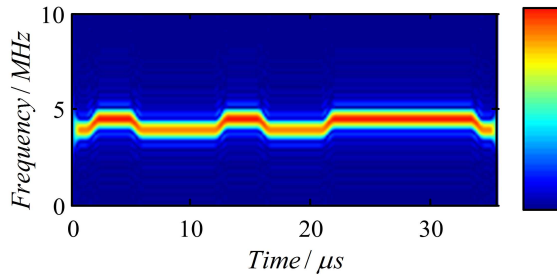


Figure 7(e) TFR of simulated SIV

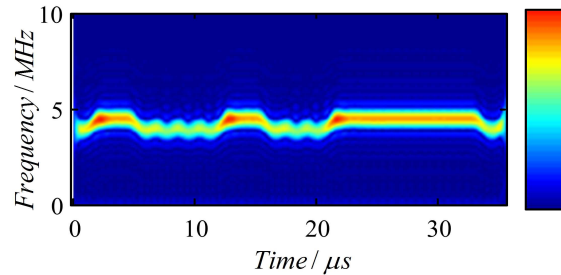


Figure 7(f) TFR of practical SIV

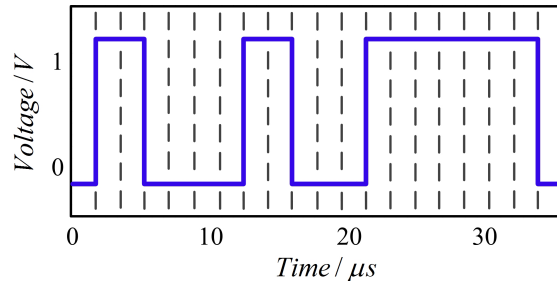


Figure 7(g) Telegram of simulated SIV

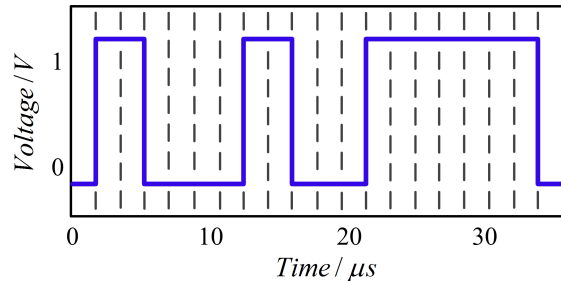


Figure 7(h) Telegram of practical SIV

Figure 7 Simulation Results And Practical Data Of Siv And Div

As shown in Figure 7(a) and 7(b) are the time-domain waveforms of SIV under simulation conditions and practical conditions respectively. It could be discovered that they are quite similar to each other no matter in aspect of the amplitude or the overall change law, in addition, the amplitude of simulated signal is fairly smooth due to its relatively ideal conditions, while the practical signal is somehow affected by the influence of noise and overshoot impulse phenomenon appears frequently on the waveform whenever the amplitude fluctuates. Spectrums of simulated signal and practical signal are displayed in Figure 7(c) and 7(d), each of them has two peaks corresponding to lower side frequency and upper side frequency respectively and the heights of peaks are also in consistency. What's demonstrated in Figure 7(e) and 7(f) are the time-frequency representations (TFR) of SIV signal obtained by employing a time-frequency analysis method named as AOK-TFR

[10]. It could be seen that as time passes, the instantaneous frequency of the signal takes alternative values between lower side frequency and upper side frequency. After demodulation and decoding, the telegram information of simulated SIV and practical SIV are extracted, as displayed in Figure 7(g) and 7(h); it is obvious that the two of them are the same, also in consistency with that of input signal, which successfully proves the validity of this FEM model and credibility of the simulation results.

5.2 Verification of DIV

In this case, Δx is changeable so that the BTM antenna is allowed to approach, pass and leave the balise, thus simulating the whole motion process of train passing balise, and the simulation results of DIV are illustrated in Figure 8(a) and 8(b), while the practical data of DIV are illustrated in parallel in Figure 9(a) and 9(b) as contrast.

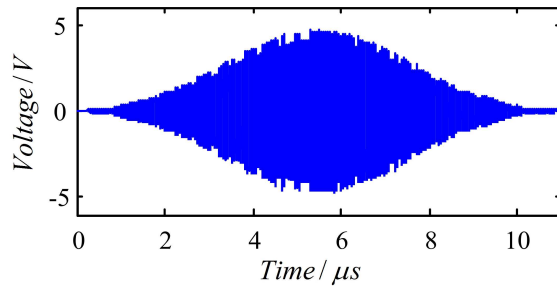


Figure 8(a) Waveform of simulated DIV

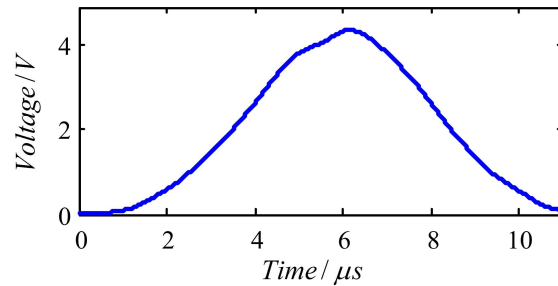


Figure 8(b) Envelope of simulated DIV

Figure 8 Waveform And Envelope Of Simulated DIV

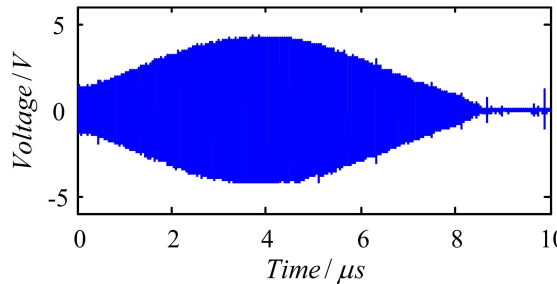


Figure 9(a) Waveform of practical DIV

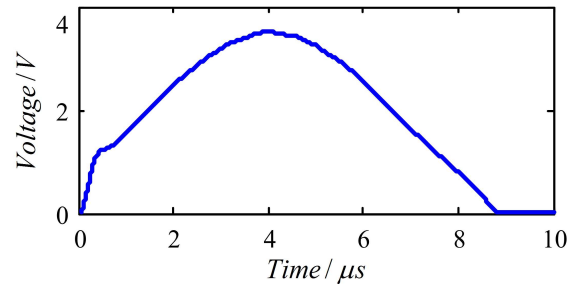


Figure 9(b) Envelope of practical DIV

Figure 9 Waveform And Envelope Of Practical DIV

Figure 8(a) and 9(a) present the time-domain waveforms of BTM DIV signals corresponding to simulation conditions and practical conditions respectively; it is observed that they share nearly the same shape resembling a standard single-peak curve. Why the amplitude of practical signal starts from a certain value attributes to a fact that the data acquisition device from which the signal is acquired has a certain threshold so that only data exceed the threshold would be recorded. What's displayed in Figure 8(b) and 9(b) are the envelopes extracted from the corresponding time-domain waveforms, and the change law of DIV could be attained by analyzing the envelopes: when the train is far away from the balise, the amplitude of DIV is pretty low, approximate to zero; as the train approaches the balise, DIV amplitude rises speedily and reaches the maximum when the train is right above the balise; with the train leaving the balise, DIV amplitude drops quickly and finally reaches the minimum.

6. CONCLUSIONS

This article proposed a finite element based method for researching the electromagnetic interaction process of BUDT in theoretical level. First, the basic structure and working principle of the system are described, based on that, the electromagnetic model of BUDT is then built by employing FEM. Later, through simulation, the electromagnetic field distribution of the process is

obtained, thus successfully simulated the dynamic balise data transmission process. Finally, contrast verification is accomplished using simulation results and practical data in two aspects, i.e., BTM SIV and BTM DIV, proving that the FEM based model is valid and the simulation results are credible, which will provide theoretical foundations for further studies regarding the optimization of balise information transmission.

ACKNOWLEDGEMENTS

This work was supported by the key project of China Ministry of Railway: "The research of basic theory of high-speed railway -- Research on basic theory of reliable transmission information of track circuit and balise in high-speed railway" (2011X021-C).

REFERENCES:

- [1] M. Sandidzadeh, A. Khodadadi, "Optimization of balise placement in a railway track using a vehicle, an odometer and genetic algorithm", *Journal of Scientific & Industrial Research*, Vol. 70, No. 3, 2011, pp. 210-214.
- [2] JF. Sevillano, J. Mendizabal, "Reliability analysis of an ERTMS on-board balise transmission equipment", *European Safety and Reliability Conference*, Reliability, Risk and



- Safety: Theory and Applications, September 7-10, 2010, pp. 2317-2324.
- [3] J Del Portillo, I. Adin, A. Villaro, "Safety analysis of the on-board front-end transceiver of the Balise Transmission Module", *Reliability, Risk and Safety: Theory and Applications*, September 7-10, 2010, pp.2013-2019.
 - [4] R. Sharma, RM. Lourde, "Crosstalk Reduction in Balise and Infill Loops in Automatic Train Control", *Proceedings of 11th International Conference on Intelligent Engineering Systems*, June 29-July 1, 2007, pp. 39-44.
 - [5] H. Zhao, S. Sun, "Dynamic characteristics modeling and adaptability research of the balise transmission module in high speed railways", *Proceedings of 12th International Conference on Computer System Design and Operation in the Railway and other Transit Systems*, August 31-September 2, 2010, pp. 475-482.
 - [6] H. Zhao, K. Tang, "The Dynamic Characteristics of Balise Transmission Module and the Assessment on Its Adaptability under High Speed Condition", *China Railway Science*, Vol. 31, No. 3, 2010, pp. 93-96.
 - [7] N. Xu, JL. Zhang, "The Crucial Techniques of Balise Onboard Test Equipment for High Speed Train", *China Railway Science*, Vol. 31, No. 4, 2010, pp. 131-137.
 - [8] Union Industry of Signaling SUBSET-036-V 2.4.1 Form Fit Function Interface Specification for Eurobalise 2007.
 - [9] Union Industry of Signaling SUBSET-085-V 2.2.2 Test Specification for Eurobalise Form Fit Function Interface Specification 2007.
 - [10] L. Zhao, J. Mu, "Fault Diagnosis Method for Jointless Track Circuit Based on AOK-TFR", *Journal of Southwest Jiaotong University*, Vol. 46, No. 1, 2011, pp. 84-91.